1D-VAR Retrieval of Temperature and Humidity Profiles from Ground-based Microwave Radiometers

Tim J. Hewison, *Member, IEEE* and Catherine Gaffard.

Abstract— A variational retrieval method is described to combine observations from microwave and infrared radiometers and surface sensors with background from short-range Numerical Weather Prediction (NWP) forecasts in an optimal way, accounting for their error characteristics. The required forward models are described. Observation errors are found to be dominated by representativeness, due to their sensitivity to atmospheric variability on smaller scales than the NWP model gird. Their effect can be reduced by evaluating this dynamically. Profiles of temperature and total water content are retrieved from synthetic data using Newtonian iteration. An error analysis shows these are expected to improve mesoscale NWP, retrieving temperature profiles with an uncertainty of <1 K up to 5 km and humidity with <40% up to 3 km, albeit both with poor vertical resolution. A cloud classification scheme is introduced to address convergence problems and constrain the retrievals. This Bayesian method can be extended to form a basis for future *Integrated Observing Systems*.

Index Terms—Atmospheric measurements, Microwave radiometry, Remote sensing, Variational methods.

I. INTRODUCTION

The retrieval of temperature and humidity profiles from passive ground-based sensors is an *ill-posed* problem, because there are an infinite number of atmospheric states that can produce a given observation vector within its uncertainty. This can be resolved by the addition of *background* data. Variational retrievals provide an *optimal* method of combining observations with a background in the form of a short-range forecast from a Numerical Weather Prediction (NWP) model which accounts for the assumed error characteristics of both. For this reason they are often referred to as *Optimal Estimation* retrievals. This is similar to the *Integrated Profiling Technique* [1], but takes its background from an NWP model instead of radiosondes and uses different control variables to concentrate on retrieving profiles of atmospheric temperature and humidity.

The variational retrieval is performed by adjusting the atmospheric state vector, $\mathbf{x}$, from the background state, $\mathbf{x^b}$, to minimize a cost function of the form [2]:

$$J(\mathbf{x}) = \left[\mathbf{x} - \mathbf{x^b}\right]^T \mathbf{B}^{-1} \left[\mathbf{x} - \mathbf{x^b}\right] + \left[\mathbf{y} - H(\mathbf{x})\right]^T \mathbf{R}^{-1} \left[\mathbf{y} - H(\mathbf{x})\right] \quad (1)$$

where $\mathbf{B}$ and $\mathbf{R}$ are the error covariance matrices of the background, $\mathbf{x^b}$, and observation vector, $\mathbf{y}$, respectively, $H(\mathbf{x})$ is the forward model operator and ^{T} and $^{-1}$ are the matrix transpose and inverse, respectively, using the standard notation of [3].

II. BACKGROUND DATA AND STATE VECTOR

The mesoscale version of the Met Office Unified Model is used to provide background data for the retrievals in the form of profiles of temperature, humidity and liquid water. The model grid points (12 km apart) are interpolated to the position of the observations. This model is initiated every six hours, including data from radiosonde stations. A short-range forecast (T+3 to T+9 hr) is used for the background, as would be available to operational assimilation schemes. This is independent of any radiosondes launched at observation time, which may be used to validate the retrievals. The background was found to have a consistent bias with respect to co-located radiosondes used in this study. This is believed to be due to the mesoscale model's limited representation of the orography. This bias was corrected empirically prior to using the background in the retrieval.

The state vector, $\mathbf{x}$, used in the retrievals is defined as the temperature and total water on the lowest 28 model levels. These extend up to 14 km, but are concentrated near the surface, where most of the radiometer's information is.

In this study the humidity components of the state vector are defined as the natural log of total water, lnq_t. (q is the specific humidity.) This control variable is a modified version of that suggested in [4], with a smooth transfer function between water vapor for $q_t/q_{sat} < 90\%$ and liquid water for $q_t/q_{sat} > 110\%$ (where q_{sat} is q at saturation.) The condensed part of the total water is further partitioned between liquid and ice fractions as a function of temperature, following [5].

This inhibits the formation of liquid water at very low temperatures. The use of total water has the advantage of reducing the dimension of the state vector, enforcing an implicit super-saturation constraint and correlation between humidity and liquid water. The use of the logarithm creates error characteristics that are more closely Gaussian and prevents unphysical retrieval of negative humidity.

The background error covariance, **B**, describes the expected variance at each level between the forecast and true state vector and the correlations between them. In this work, **B** was taken from that used to assimilate data from satellite instruments operationally at the Met Office. It could also be calculated from the differences between the radiosondes and background from the mesoscale forecasts over an extended period. This **B** is defined in terms of temperature and lnq. It is assumed that the error characteristics of lnq_t are similar to those of lnq as liquid water is not measured by the radiosondes. This method provides a worst-case estimate of **B** as it includes contributions from the radiosonde error and the representativeness errors. The diagonal components of **B** are shown for reference in Fig. 4.

III. OBSERVATIONS

This study uses observations from the Radiometrics TP/WVP-3000 microwave radiometer [6]. This has 12 channels: seven in the oxygen band 51-59 GHz, which provide information primarily on the temperature profile and five between 22-30 GHz near a water vapor line, which provide cloud and humidity profile information. This radiometer includes sensors to measure pressure, temperature and humidity at ~1 m above the surface. The pressure is taken as a fixed reference from which geopotential height is calculated at other pressure levels via the hydrostatic equation. The instrument's integral rain sensor is used to reject periods which may be contaminated by scattering from precipitation, as this is not included in the forward model and emission from raindrops on the radome, which may bias the calibration. This radiometer incorporates an optional zenith-viewing infrared radiometer (9.6-11.5 μm) to provide information on the cloud base temperature.

In this study the observation vector, **y**, is defined as a vector of the zenith brightness temperatures (T_b) measured by the radiometer's 12 channels, with additional elements for the surface temperature and humidity (converted to lnq) and the infrared brightness temperature (T_{ir}).

The observation error covariance, **R**, has contributions from the radiometric noise (**E**), forward model (**F**) and representativeness (**M**) errors ($R = E + F + M$).

The radiometric noise, **E**, can be evaluated as the covariance of the T_bs measured while viewing a stable scene (such as a liquid nitrogen target) over a short period (~30 min). This term is approximately diagonal – i.e. the channels

are independent – with diagonal terms ~(0.1-0.2 K)^2.
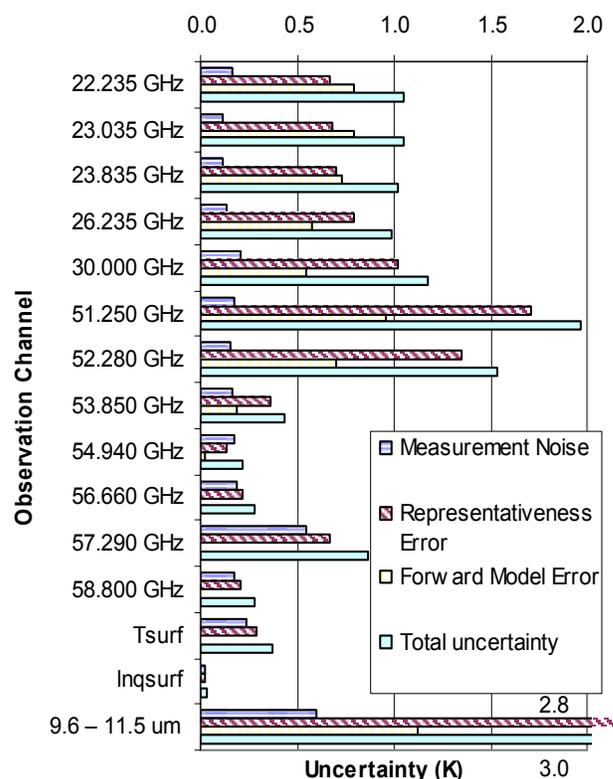
Fig. 1. Diagonal components of Observations Error Covariance Matrix, **R**.

The representativeness error, **M**, allows for the radiometer's sensitivity to fluctuations on smaller scales than can be represented by the NWP model. It is possible to estimate **M** by studying the fluctuations in the radiometer's signal on typical time scales taken for atmospheric changes to advect across the horizontal resolution of the NWP model. In the case of the mesoscale model with a 12 km grid, a time scale of 1200 s was chosen to represent a typical advection timescale. The r.m.s. difference in brightness temperatures measured over this time scale was used to calculate **M**. This showed strong correlation between those channels sensitive to liquid water, water vapor and temperature, respectively. The liquid water and humidity terms were found to vary by an order of magnitude, depending on the atmospheric conditions. The average values calculated over a 7 day period of dry conditions with variable cloud amounts were taken to be typical. The representativeness term evaluated in this way dominates the observation error covariance matrix, with terms ~(0.2-2.5 K)^2. (This method also implicitly includes the radiometric noise.)

The representativeness error has also been evaluated dynamically, based on the time series of observations within a 1 hour window around each observation used for retrieval. It is hoped that this technique will allow the observation errors to be reduced in periods of atmospheric stability, when more confidence can be placed that the radiometer observations are

representative of the model's state. Early trials with real data have produced more stable retrievals with similar characteristics to using a fixed value of **E**.

The magnitude of the diagonal components of each term of **R** is shown in Fig. 1 for the 12 channels of the microwave radiometer, surface temperature and humidity sensors (as dimensionless *lnq*) and infrared radiometer.

IV. Forward Model and its Jacobian
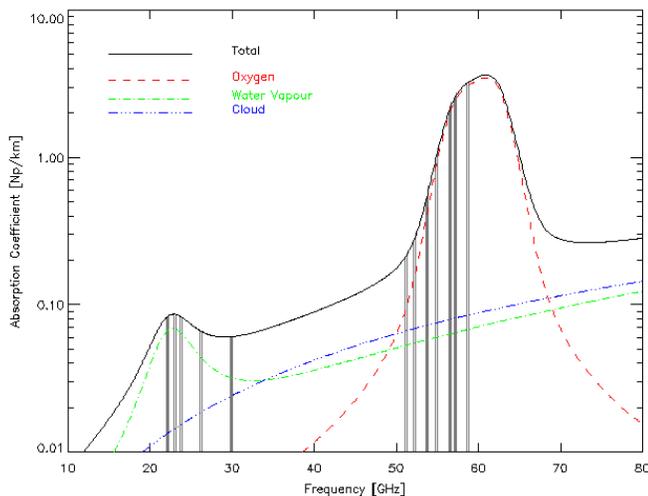
Fig. 2. Atmospheric absorption spectrum for typical surface conditions: T=288.15 K, p=1013.25 hPa, RH=100%, L=0.2 g/m^3 following [5]. Line styles show total absorption coefficient and contribution from oxygen, water vapour and cloud according to the legend. Grey vertical bars indicate the passbands of the Radiometrics TP/WVP-3000 microwave radiometer.

A forward model, $H(\mathbf{x})$, is needed to transform from state space to observation space. For the microwave radiometer, each channel's T_b is calculated at an equivalent monochromatic frequency [9] using the radiative transfer equation to integrate down-welling emissions from each atmospheric layer between model levels using a standard absorption model [5], which was found to have small biases in these channels [10]. The forward model for the surface temperature and humidity sensors is trivial – a 1:1 translation to the lowest level of the state vector, $\mathbf{x}$. A simple forward model defines T_{ir} as the temperature of the lowest level with any cloud. A more sophisticated radiative transfer model has also been developed for T_{ir} which accounts for absorption by atmospheric water vapor and the finite extinction in liquid water cloud, assigning extinction coefficients of 7.2 Np/km.(kg/m^3)$^{-1}$ [11] and 0.02 Np/km.(kg/kg)$^{-1}$ respectively. This model was found to give more Gaussian error characteristics, due to having less abrupt transitions.

The *Jacobian* is the matrix of the sensitivity of the observation vector, $\mathbf{y}$, to perturbations of each element of the state vector, $\mathbf{x}$, $\mathbf{H}=H'(\mathbf{x})=\partial\mathbf{y}/\partial\mathbf{x}$. It is needed to minimize the cost function (see section VI). In this case, **H** is calculated by 'brute force' – each level of the state vector, $\mathbf{x}$, is perturbed by

1 K in temperature or 0.001 in lnq_t. The magnitude of these perturbations was selected to ensure linearity of **H**, while preventing numerical errors due to truncation.

However, to speed up the calculation, a *Fast Absorption Predictor* model is used to calculate the absorption in each level below 100 hPa as a third order polynomial function of pressure, temperature and q following [1]. This introduces an additional random error in the calculation of T_b approximately as large as the forward model error contribution above.

H is only calculated for levels between 0-8 km, corresponding to the maximum range of likely impact from the radiometer data. For levels above this, **H**=0.
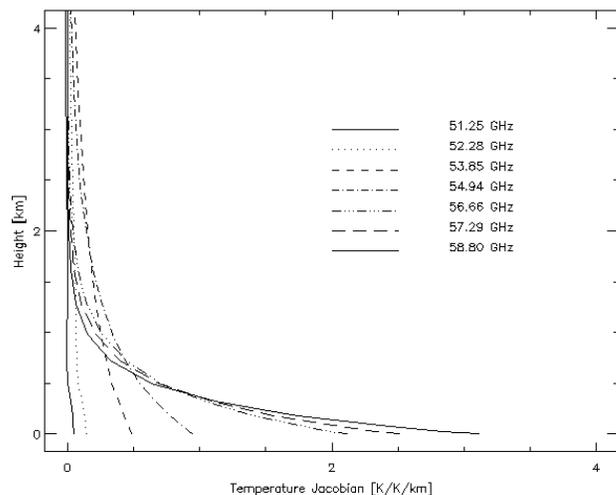
Fig. 3. Temperature Jacobians of 51-59 GHz channels of Radiometrics TP/WVP-3000, scaled by model layer thickness,Δz: $\mathbf{H}/\Delta z =(\partial\mathbf{y}/\partial\mathbf{x})/\Delta z$.

V. Error Analysis

An estimate of the uncertainty on the retrieved profile can be derived by assuming the errors are normally distributed about the solution and that the problem is only moderately non-linear. In this case, the error covariance matrix of the analysis, **A**, is given by [2]:

$$\mathbf{A} = \left(\mathbf{H}_i^T \mathbf{R^{-1}} \mathbf{H}_i + \mathbf{B^{-1}} \right)^{-1} \qquad (2)$$

where $\mathbf{H}_i$ is evaluated at the solution (or final iteration).

Although **A** depends on the reference state through $\mathbf{H_i}$, it has been evaluated for different combinations of instruments for a US standard atmosphere in Fig. 4. This shows error in the temperature profile retrieved from the radiometer is expected to approach 0.3 K near the surface, but increases with height, to exceed 1 K above 5 km. For the humidity profile, **A** varies greatly with $\mathbf{x}$. In this case the retrieval's *lnq* error increases from 0.1 (~10%RH) near the surface to 0.4 (~40%RH) by 3 km. This presents a substantial improvement on the background, which exceeds 1 K at all levels, and the surface sensors alone, which only influence the lowest 500 m, but falls short of the

radiosonde's accuracy above 1 km for both *T* and *lnq*. The radiosonde's **R** used here is a diagonal matrix, dominated by representativeness errors and may not be perfect. However, the radiometer provides much more frequent observations than radiosondes can, reducing errors of representativeness applying their data to analysis at arbitrary times.
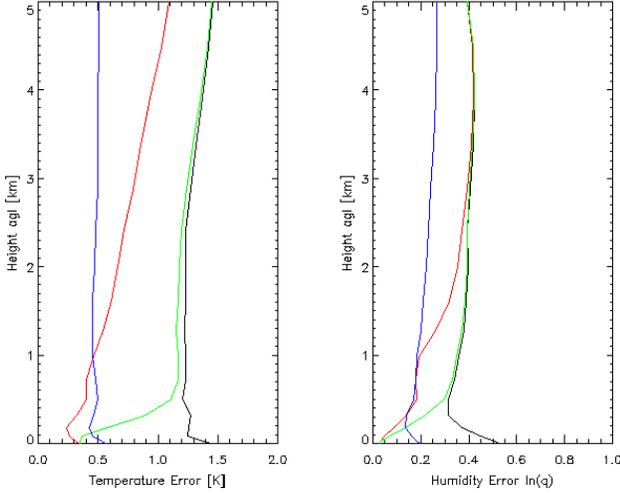
Fig. 4. Background error covariance matrix from mesoscale model, **B** (black) and analysis error covariances matrices, **A**, with surface sensors only (green), radiometers and surface sensors (red), and radiosonde only (blue). Plotted as square root of the diagonal components for the lowest 5km of temperature [K] and humidity (*lnq*) [dimensionless].
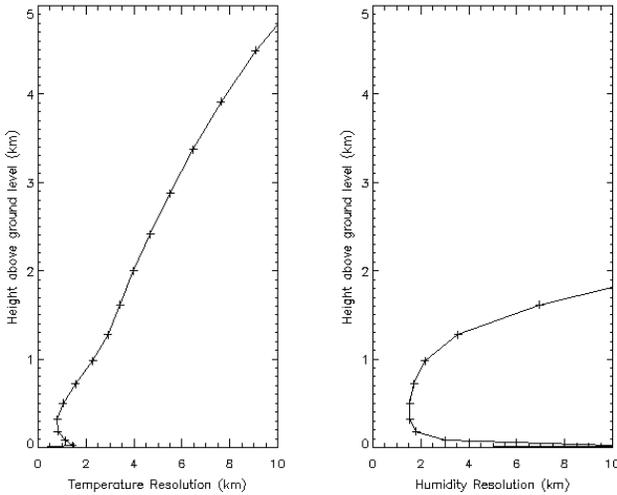
Fig. 5. Vertical Resolution of temperature and humidity (*lnq*) retrievals.

However, **A** only tells part of the story. The other important aspect of the retrieval's performance is the vertical resolution – i.e. its ability to resolve a perturbation in state space. One simple, robust definition of the vertical resolution is the inverse of the trace of the *averaging kernel matrix* [2], following the concept of data density [12]. This is evaluated in Fig. 5, which shows that the vertical resolution of temperature profiles increases with height, from ~1 km near the surface, as approximately twice the height from 0.5-4 km.

For *lnq*, it increases from 1.5 km near the surface, as approximately 4 times the height above 1.5 km. However this definition tends to over-estimate the vertical resolution by a factor of ~2 compared to other methods [13], [14].

VI.   MINIMIZATION OF COST FUNCTION

Variational retrievals are performed by selecting the state vector that minimizes a cost function in the form of (1). For linear problems, where **H** is independent of **x**, this can be solved analytically. However, the retrieval of profiles of temperature above ~1 km and humidity is moderately non-linear, so the minimization must be conducted numerically. This can be achieved using the Gauss-Newton method [2], by applying the following analysis increments iteratively:

$$\mathbf{x}_{i+1} = \mathbf{x}_i + \left(\mathbf{B}^{-1} + \mathbf{H}_i^{\mathbf{T}} \mathbf{R}^{-1} \mathbf{H}_i \right)^{-1} \cdot$$
$$\left[\mathbf{H}_i^{\mathbf{T}} \mathbf{R}^{-1} \left(\mathbf{y}^{\mathbf{o}} - H(\mathbf{x}_i) \right) - \mathbf{B}^{-1} \left(\mathbf{x}_i - \mathbf{x}^{\mathbf{b}} \right) \right] \tag{3}$$

where $\mathbf{x}_i$ and $\mathbf{x}_{i+1}$ are the state vector before and after iteration i, **B** and **R** are the error covariance matrices of the background and observations, respectively, $\mathbf{H}_i$ is the Jacobian matrix at iteration, i.

This is iterated until the following convergence criteria [2] is satisfied, based on a χ^2 test of the residuals of $\mathbf{y}^{\mathbf{o}}$-$H(\mathbf{x})$:

$$\left[\left(H(\mathbf{x}_{i+1}) - H(\mathbf{x}_i) \right) \right]^T \mathbf{S}_{\delta\mathbf{y}}^{-1} \left[\left(H(\mathbf{x}_{i+1}) - H(\mathbf{x}_i) \right) \right] << m \tag{4}$$

where $\mathbf{S}_{\delta\mathbf{y}}$ is the covariance matrix between $\mathbf{y}^{\mathbf{o}}$ and $H(\mathbf{x}_i)$ and m is the dimension of $\mathbf{y}^{\mathbf{o}}$ (number of observations).

This typically takes 3-10 iterations, each requiring ~0.25 s of CPU time on a 2.4 GHz Pentium IV using the *Fast Absorption Predictor* model.

Upon convergence the retrieved state vector, $\hat{\mathbf{x}}$, is tested for statistical consistency with $\mathbf{x}^{\mathbf{b}}$ and **B** by calculating the value:

$$\chi^2 = \left(\hat{\mathbf{x}} - \mathbf{x}^{\mathbf{b}} \right) \mathbf{B}^{-1} \left(\hat{\mathbf{x}} - \mathbf{x}^{\mathbf{b}} \right) \tag{5}$$

Retrievals with a χ^2>20 were rejected, based on the expected distribution of χ^2 for 99% of a population with 8 degrees of freedom. While it is recognized that this over-estimates the true number of degrees of freedom, it is important not to use a test that is too restrictive as we are particularly interested in cases where the background does not provide an accurate estimate of the truth. The choice of χ^2 threshold was found not to be critical, as it had a small influence on the statistics of the retrievals.

VII.   EXAMPLE 1D-VAR RETRIEVALS

Fig. 6 shows an example of a 1D-VAR retrievals using synthetic observations, generated to be consistent with **R**. These are based on a real radiosonde profile for Camborne (UK) at 11:21 on 9/12/2004 and NWP background profile from a 5 hr forecast, valid 21 minutes earlier. This case was

selected because the model had forecast the inversion ~200 m too low and overestimated the humidity by a factor of ~2 over the whole profile. The retrieval was repeated for 100 such sets of observations, 83% of which converged within an average of 9.1 iterations. The retrieved profiles are closely clustered with typical standard deviations of 0.2-0.5 K in temperature and 0.0-0.1 in *lnq*, showing they are relatively robust in the presence of observation noise. In all cases, the retrieval thins the cloud and gives profiles closer to the truth than the background. However, the structure of **B** makes it impossible for the retrieval to move a misplaced feature in the vertical.
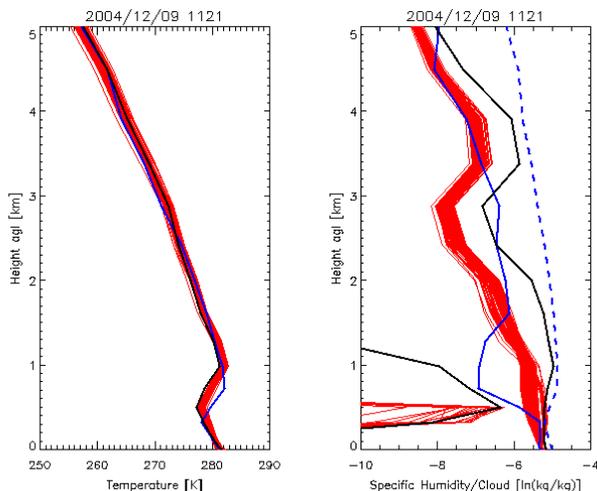
Fig. 6. Example retrievals (red) with 100 synthetic observations, with profiles between NWP model background (black) and truth (blue). Left panel shows temperature profiles. Right panel shows profiles of humidity (*lnq*) and liquid water (*lnq_l*) and specific humidity at saturation (dotted line). Retrievals improve background state, but fail to move inversion in vertical.

VIII. CLOUD CLASSIFICATION SCHEME

Examination of the performance of the retrieval scheme shows there are often problems when profiles approach the threshold of cloud formation – the residuals will often oscillate without reaching convergence. Attempts have been made to address this by implementing the Levenberg-Marquardt [2] method of minimization, which adjusts the size of the increment at each iteration to change from the classic Gauss-Newton method towards the method of steepest decent, according whether the previous iteration has improved the χ^2 value of $\mathbf{x}_i$. These investigations are continuing.

Convergence problems in borderline cloud conditions can also be caused by the error characteristics of T_{ir}, which can be highly non-Gaussian. This has been addressed by introducing a cloud classification as a pre-processing step to the retrieval, based on a threshold of the infrared brightness temperature, T_{ir}. If the observed (or synthetic) $T_{ir} > \min\{T_{amb}-40\text{ K}, 223\text{ K}\}$, the profile is classified as *cloudy* and the retrieval proceeds as described above. Otherwise, the profile is classified as *clear* and the control variable changed from the logarithm of the total water, lnq_t to that of the specific

humidity, *lnq*. In this case, an addition term [15] is added to the cost function, modified to prevent saturation or super-saturation. In *clear* cases, T_{ir} will have no impact on the retrievals and the representativeness term, which dominates **R,** can be reduced by re-evaluating it in only clear sky conditions, as for optically thin channels, this is dominated by cloud variability. This reduction allows the retrievals to be more accurate in clear conditions. *Rainy* observations are rejected.

IX. STATISTICS OF 1D-VAR RETRIEVALS

1D-VAR retrievals were performed on an extended dataset of radiosonde profiles from Camborne during winter 2004/05, using synthetically generated observations and backgrounds, consistent with **R** and **B**, respectively. The statistics for the *cloudy* cases, shown in Fig. 7, are in excellent agreement with the expected performance from the error analysis, albeit with a poor convergence rate (77/179 cases). However, the retrieved temperature profiles do show a small, but consistent bias at higher levels. This may be introduced due to remaining non-linearity in the retrieval [16].
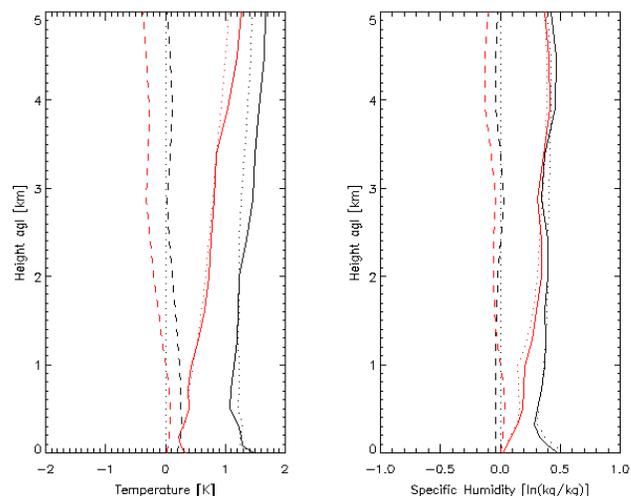
Fig. 7. Statistics of 1D-VAR retrievals using synthetic observations and background for 77 cloudy cases from Camborne, UK during winter 2004/05. Solid lines show standard deviation of difference between retrieved and sonde profiles. Dashed lines show bias. Diagonal terms of error covariances are shown as dotted lines for the analysis, **A**, black lines for the background, **B.** Red lines show the statistics of the cloudy 1D-VAR retrieval.

The retrieved values of Integrated Water Vapor (IWV) were also compared to the radiosonde values. These were found to be good, with a small bias and a standard deviation of 0.63 kg/m^2 (compared to the corresponding value for synthetic backgrounds, 2.38 kg/m^2). This compares favorably with other methods, which have been shown to retrieve IWV from microwave radiometer observations with an accuracy of better than 1.0 kg/m^2 compared to radiosondes in mid-latitude winter [17]. This implies that the retrievals do not need an additional constraint in the cost function to force the IWV to match that retrieved by a simpler method.

X. Conclusions and Future Work

A 1-D variational retrieval has been developed to allow observations from ground-based microwave and infrared radiometers and surface sensors to be combined with a background from an NWP model in an optimal way, which accounts for their error characteristics. This has been shown to be advantageous over methods taking their background from statistical climatology [18]. This has been used to retrieve profiles of temperature, humidity and cloud using a novel total water control variable.

The observation errors for channels sensitive to cloud were dominated by representativeness errors. To reduce their impact, these can be evaluated dynamically. However, convergence problems were encountered, partially due to the non-Gaussian error characteristics of the infrared observations. A cloud classification scheme has been introduced to address this and help constrain the retrievals. Other minimization schemes and convergence criteria may also help.

The 1D-VAR retrievals also have the advantage of providing an estimate of the error on the retrieved profile. Error analysis has shown the microwave radiometer improves the NWP background, retrieving temperature profiles with <1 K uncertainty up to 5 km and humidity with <40% uncertainty below 3 km. However, the vertical resolution of the retrieved profiles is poor and degrades with height. Furthermore, the retrievals were not able to move a misplaced feature in the background profile.

The variational method allows different instruments to be combined if their observations' forward model operator and error estimates are available. This provides a basis for the development of *Integrated Observing Systems*. In the future the 1D-VAR retrievals will be extended to include observations from other instruments, such as the cloud base height from a ceilometer, Integrated Water Vapor from GPS, cloud base/top from cloud radar and boundary layer height from a wind profiler.

Assimilation of these observations could improve mesoscale Numerical Weather Prediction (NWP), especially in the boundary layer and cloud properties. However, to fully exploit the high time resolution available from ground-based instruments will require 4-Dimensional Variational Assimilation (4D-VAR).

References

[1] U. Löhnert, S. Crewell, C. Simmer, "An Integrated Approach toward Retrieving Physically Consistent Profiles of Temperature, Humidity, and Cloud Liquid Water", J. Appl. Meteorology 2004 43: 1295-1307

[2] C. D. Rodgers, *Inverse Methods for Atmospheric Sounding: Theory and Practice*, World Scientific Publishing Co. Ltd., 2000.

[3] K. Ide, P. Courtier, M. Ghil and A. C. Lorenc, "Unified Notation for Data Assimilation: Operational, Sequential and Variational," J. Meteor. Soc. Japan, Vol. 75, No. 1B, pp. 181-189, 1997

[4] G. Deblonde and S. J. English, "One-Dimensional Variational Retrievals From SSMIS Simulated Observations", J. Appl. Meteorology, 2003 42: 1406-1420

[5] D. C. Jones, "Validation of scattering microwave radiative transfer models using an aircraft radiometer and ground-based radar," PhD Thesis, University of Reading, Dept. of Meteorology, 1995.

[6] R. Ware, F. Solheim, R. Carpenter, J. Gueldner, J. Liljegren, T. Nehrkorn and F. Vandenberghe, "A multi-channel radiometric profiler of temperature, humidity and cloud liquid," Radio Science, 38, No.4, 2003, pp.8079-8092.

[7] P. W. Rosenkranz, "Water vapor microwave continuum absorption: A comparison of measurements and models," Radio Science, Vol.33, No.4, 1998, pp.919-928 *and subsequent correction* in Radio Science, Vol.34, No.4, 1999, p.1025

[8] H. J. Liebe, G. A. Hufford, M. G. Cotton, "Propagation modeling of moist air and suspended water/ice particles at frequencies below 1000GHz, " AGARD 52nd Specialists' Meeting of the Electromagnetic Wave Propagation Panel, Paper No. 3/1-10, Palma de Mallorca, Spain, 17-21 May 1993.

[9] D. Cimini, T. J. Hewison, L. Martin, "Comparison of brightness temperatures observed from ground-based microwave radiometers during TUC," Meteorol. Zeitschrift, Vol.15, No.1, 2006, pp.19-25.

[10] T. J. Hewison, D. Cimini, L. Martin, C. Gaffard and J. Nash, "Validating clear air absorption model using ground-based microwave radiometers and vice-versa," Meteorologische Zeitschrift, Vol.15, No.1, 2006, pp.27-36.

[11] P. Chýlek and V. Ramaswamy, "Simple Approximation for Infrared Emissivity of Water Clouds," J. Atmosph. Sci., Vol..39, 1982, pp.171-177

[12] R. J. Purser and H.-L. Huang, "Estimating Effective Data Density in a Satellite Retrieval or an Objective Analysis", J. Appl. Meteorology, Vol.32, No.6, 1993, pp.1092-1107.

[13] A. Collard, "Notes on IASI performance", 1998, NWP Technical Report No.56, Met Office, UK. Available from http://www.metoffice.gov.uk/

[14] J. C. Liljegren, S. A. Boukabara, K. Cady-Pereira and S. A. Clough, "The Effect of the Half-Width of the 22-GHz Water Vapor Line on Retrievals of Temperature and Water Vapor Profiles with a Twelve-Channel Microwave Radiometer," IEEE Trans. Geoscience and Remote Sensing, Vol.43, No.5, May 2005, pp.1102-1108.

[15] L. Phalippou, "Variational retrieval of humidity profile, wind speed and cloud liquid-water path with SSM/I: Potential for numerical weather prediction," Q. J. Royal Meteorol. Soc., Vol.122, No.530, Jan 1996, pp.327-355.

[16] J. R. Eyre and A. D. Collard, "The effects of nonlinearity on retrieval errors: implications for the interpretation of advanced infra-red sounder data," Tech Proc 10th Int TOVS Study Conf; Boulder, USA; 27 January - 2 February 1999; Eds: J Le Marshall and J D Jasper; Bureau of Meteorology Research Centre, Australia; pp.191-202 (1999).

[17] L. Martin, C. Mätzler, T. J. Hewison and D. Ruffieux, "Intercomparison of integrated water vapour measurements," Meteorologische Zeitschrift, Vol. 15, No. 1, 1-8 (February 2006).

[18] D. Cimini, T. J. Hewison, L. Martin, J. Güldner, C. Gaffard and F. S. Marzano, "Temperature and humidity profile retrievals from ground-based microwave radiometers during TUC," Meteorologische Zeitschrift, Vol. 15, No. 5, 1-12 (February 2006).